# CHAPTER 6
# NUMERICAL HEAT TRANSFER ANALYSIS AND THERMAL OPTIMIZATION OF INFANT INCUBATOR SYSTEMS

*Muhammad Faiz Md Shakhih[1], Mohamad Al Amin bin Mohamed[1], Congo Tak Shing Ching[3], Kahar Osman[2], Mohamad Ikhwan Jamaludin[1*], and Nofrizalidris Darlis[4]*

[1]Department of Biomedical Engineering and Health Sciences, Faculty of Electrical Engineering, Universiti Teknologi Malaysia, 81310 Johor, Malaysia

[2]Faculty of Mechanical Engineering, Universiti Teknologi Malaysia, 81310 Johor, Malaysia.

[3]Graduate Institute of Biomedical Engineering,
[4]Department of Mechanical Engineering Technology, Faculty of Engineering Technology, Universiti Tun Hussein Onn Malaysia, Pagoh Higher Education Hub, KM 1, Jalan Panchor, 84600 Pagoh, Muar, Johor, Malaysia

## 6.1 INTRODUCTION

### 6 .1 .1 Recent Studies on CFD for Thermoneutral Care in Closed Incubators

Neonatal incubators aim to maintain a thermoneutral environment. However, infants still lose heat through convection and radiation when internal airflow is poorly organized or when interior surfaces remain cooler than the air. These risks are most pronounced in preterm infants and in transport conditions. Recent studies therefore treat the incubator as a coupled thermal–fluid system, where outcomes depend on geometry (hood curvature, corners), air-distribution (inlet/outlet placement, jet direction), and operating set-points (air temperature, flow rate), not merely on a single thermostat reading [1]. This framing motivates the present work's focus on hood shape and supply/return strategy, as well as how these choices influence temperature fields and velocity organisation within the chamber. As a baseline, the canonical circulation loop within the chamber jet supply, wall-guided return, and outlet extraction is shown in Figure 6.1 (adapted from the thesis schematic). This picture anchors later discussion of corner eddies, jet impingement, and stratification [2].

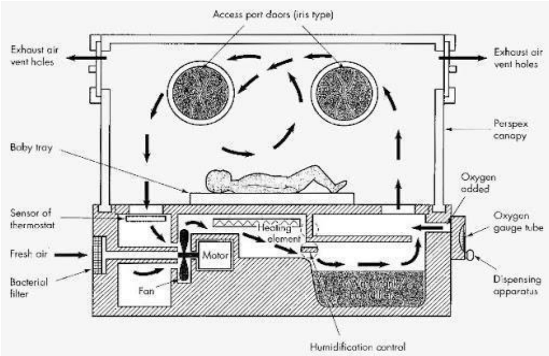


**Figure 6.1:** Air circulation inside an infant incubator

### 6 .1 .2 Neonatal thermal physiology and the thermoneutral target

Preterm infants exhibit a high surface-area-to-mass ratio, reduced skin barrier, and immature vasomotor control; consequently, small spatial variations in air temperature or mean radiant temperature can perturb heat balance. Operative temperature, the combined effect of air and radiation, therefore better predicts thermal stress than air temperature alone, and design/controls should aim to flatten mean radiant temperature around the infant [3]. Recent modeling and manikin studies provide segment-wise heat-transfer descriptors and show that air-only metrics can mislead if the radiant field is non-uniform [4].

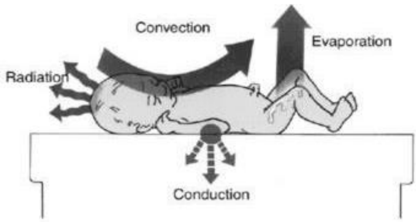


**Figure 6.2:** Heat-transfer pathways for a neonate in a closed incubator (conduction, convection, radiation, evaporation) with emphasis on wall-cooling effects

In closed incubators operating with modest flow, convection and radiation dominate dry heat exchange; radiation is strongly affected by the mean radiant temperature of hood/wall panels, while convection depends on local velocity and turbulence patterns near exposed regions (head, chest). Segmental correlations for convective and radiative coefficients inside incubators confirm that air temperature set-point and local flow organization jointly govern losses [5].

### 6.1 .3 Enclosure geometry, air distribution, and access ports

CFD evidence shows that hood curvature and vent layout are first-order determinants of flow topology: rounded (semicircular) ceilings suppress corner vortices, reduce jet impingement on the face/torso, and yield more uniform temperature fields than sharp-cornered [6]. Operational features matter, too. Access ports introduce a design–control trade-off: opening ports enhances exchange but depresses internal temperature; covers maintain central temperature but can cause vertical stratification unless return paths are guided [7]. Early and later device documents/patents illustrate how diffuser placement and return paths attempt to homogenize the field [8].

### 6.1.4 Computational modelling for incubator design

Computational fluid dynamics (CFD) supports rapid iteration on enclosure geometry and control concepts. Typical workflows pair CAD with meshing and a turbulence closure such as SST k–ω, which handles near-wall separation and recirculation around complex infant shapes; the finite-volume framework is standard in such analyses [9]. Recent incubator CFD studies adopt SST k–ω and report improved agreement with manikin/segment-wise benchmarks over simpler models [10]. Validation strategies increasingly use 3D-printed thermal manikins with segmental heating to compare predicted vs. measured surface temperatures and heat fluxes under controlled set-points [11].

Thermoelectric actuation and model-based control offer tighter temperature stability with lower acoustic/vibration loads than conventional resistive heating, complementing geometric improvements [12]. Historical tools such as HeatBalance and related software illustrate earlier attempts to match set-point and humidity to infant heat balance [13], while clinical guidance underscores the risk of thermal stress and the need for systematic control [14]. Recent evidence converges on three needs: geometry flow co-design to suppress corner vortices and draft; radiant-field uniformity to stabilize operative temperature; and systematic validation with manikins/segment-wise benchmarks under realistic set-point changes [15]. However, few studies compare multiple hood profiles under identical boundary conditions while also quantifying velocity-field stability alongside infant-surface uniformity a gap addressed in the present thesis design–simulation framework.

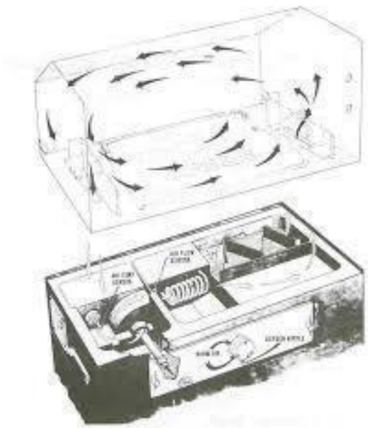

**Figure 6.3:** Typical incubator inlet (side) and outlet (top/bottom) arrangement that drives the internal recirculation loop; note implications for jet direction and return paths.

## 6.2 METHODOLOGY

This section outlines the methodology adopted for the design and evaluation of an infant incubator using computational modelling and simulation. A parametric representation of a newborn was constructed based on anthropometric measurements and validated against standard medical data to ensure physiological relevance. The incubator and infant geometries were subsequently developed for computational fluid dynamics (CFD) analysis using Solidworks and fluent, enabling the controlled study of airflow and heat transfer within a virtual environment. The methodological framework encompassed three key stages: model construction, mesh generation, and numerical simulation. In this approach, the incubator chamber was treated as a coupled thermal-fluid system, where convective airflow, conductive transfer through structural walls, and thermal interaction with the infant surface were simultaneously considered. Thermal and fluid dynamic behaviors, including heat transfer across the infant surface and airflow distribution within the incubator chamber, were analyzed to assess the performance of different design configurations and to provide insights into optimal design features that enhance thermal uniformity and infant comfort.

### 6.2.1 Model Development

The development of the incubator model began with the establishment of the infant geometry. Anthropometric measurements of a newborn-sized doll were taken and validated with standard medical data. These measurements provided the reference dimensions for creating a parametric newborn model, which was positioned within the incubator chamber, as shown in Figure 6.4.

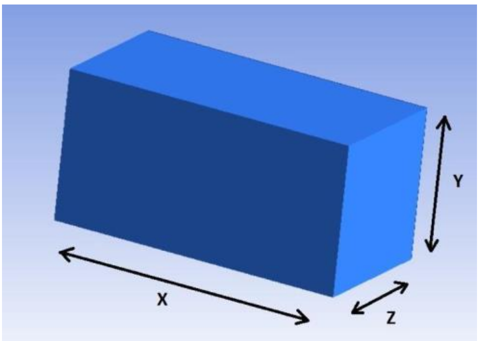


**Figure 6.4:** Newborn measurements

The incubator geometry was then constructed using SolidWorks, where the infant, the chamber walls, and the positions of air inlet and outlet were defined. The sketching process formed the basis for generating a three-dimensional representation of the system Figure 6.5

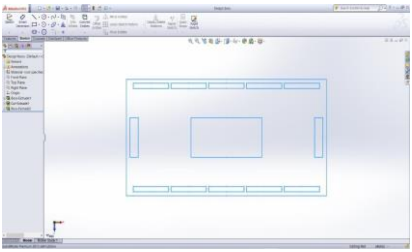

(a)

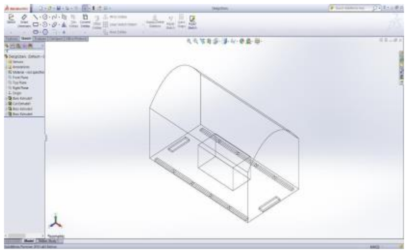

(b)

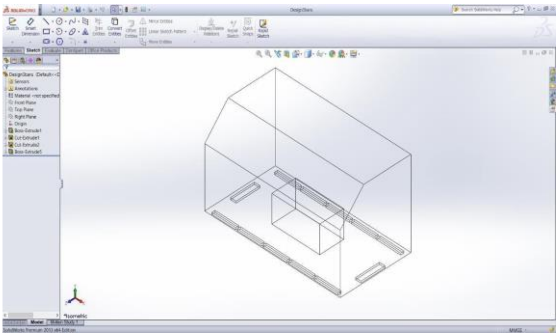

(c)

**Figure 6.5:** (a) Rectangular hood design; (b) Semicircular hood design; (c) Trapezoidal hood design

The final models provided a set of geometries suitable for subsequent computational analysis. These models served as the foundation for meshing and CFD simulations, as described in the following sections.

### 6.2.2 Meshing Process

Before simulation, the incubator models were discretized into smaller computational elements through meshing in Fluent. This process divides the geometry into nodes and components, enabling numerical calculations of airflow and heat transfer within the chamber. A six-node wedge element structure with local refinement was applied to enhance accuracy, particularly around the infant model and air passages where flow variations are most significant. Each of the three hood designs: rectangular, semicircular, and trapezoidal; was meshed separately. Representative examples of the meshed domains are shown in Figure 6.6.

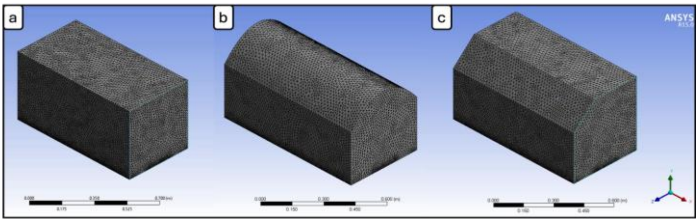

**Figure 6.6:** Meshed hoods: (a) rectangular, (b) semicircular, (c) trapezoidal.

The number of nodes and elements varied slightly between designs due to differences in surface geometry. As summarized in Table 6.1, the rectangular hood produced the highest element count, while the semicircular hood required the fewest. These variations were considered acceptable, as mesh independence testing confirmed that all models produced stable and reliable results.

**Table 6.1:** Mesh Parameters for Different Hood Designs.

| Design | Nodes | Elements |
|---|---|---|
| Rectangular Hood | 107,048 | 585,481 |
| Semicircular Hood | 99,494 | 542,232 |
| Trapezoidal Hood | 103,308 | 563,923 |

This meshing stage ensured that the computational domains were sufficiently refined for accurate CFD simulation while maintaining computational efficiency. The finalized meshes were then used as the basis for defining boundary conditions and running the simulations described in the next section.

### 6.2.3 Numerical Modelling

The CFD simulations were designed to evaluate three main aspects of incubator performance:

1. Thermal distribution across the infant's skin,
2. Airflow direction within the incubator chamber, and
3. Air velocity under varying inlet conditions.

These parameters are critical for assessing thermal comfort and uniformity, which directly influence the effectiveness of incubator design.

### 6.2.4 Boundary and Material Conditions

The simulation setup began by defining the physical models in Fluent. The k–ω SST turbulence model was selected, as it provides reliable predictions for near-wall flows and complex internal airflow complex as in Figure 6.7

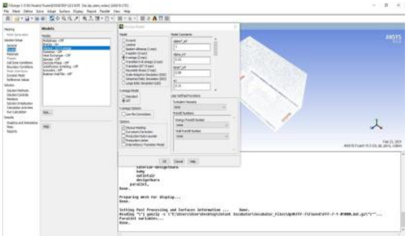

(a)

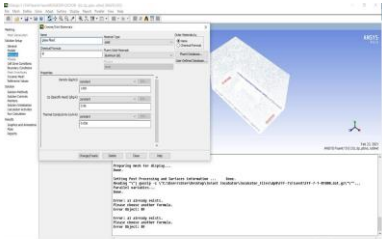

(b)

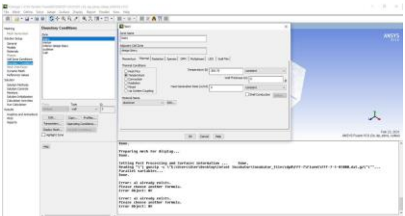

(c)

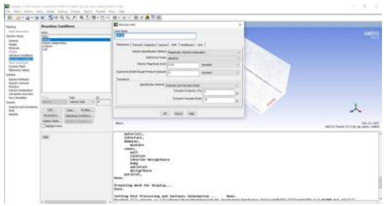

(d)

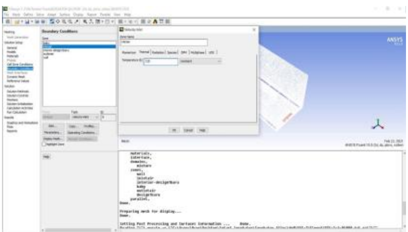

(e)

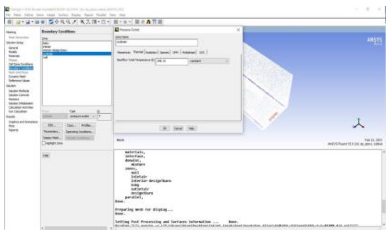

(f)

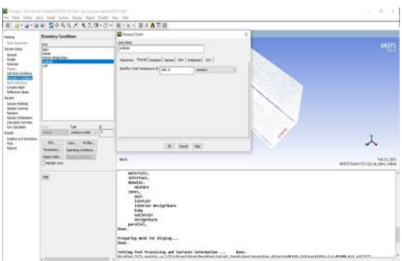

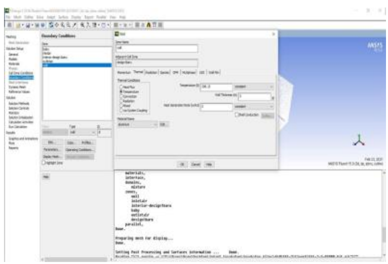

**Figure 6.7:** Simulation setup (a) Viscous model selection; (b) Wall material settings; (c) Infant body temperature setting (d) Inlet velocity magnitude setting; (e) Inlet temperature setting; (f) Inlet temperature setting; (g) Outlet condition at room temperature; (h) External wall condition

## 6.2.5 Solution Initialization and Run Settings

Simulations were run for 1000 iterations, which ensured numerical convergence and stability. The solver iteratively calculated the distribution of airflow and heat transfer until consistent results were obtained Figure 6.8.

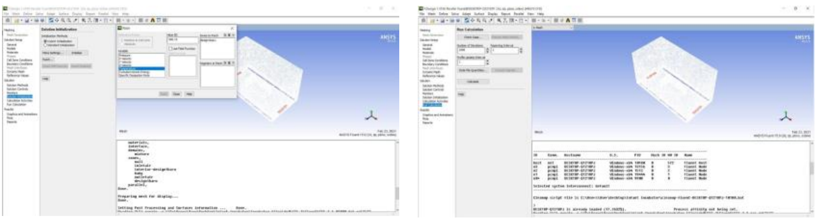

(a) (b)

**Figure 6.8:** (a) Solution initialization; (b) Simulation run with 1000 iterations

In summary, the CFD setup incorporated appropriate turbulence modelling, realistic thermal boundary conditions, and iterative convergence criteria. By controlling inlet temperature and velocity, the simulations enabled a systematic evaluation of airflow and heat distribution for the three hood designs. These results formed the basis for performance comparison, discussed in the following chapter.

## 6.3 RESULTS AND DISCUSSION

The performance of three hood configurations; rectangular, semicircular, and trapezoidal, was evaluated at two inlet temperatures (310 K and 315 K). For each case, the simulations produced data on temperature distribution, convective heat flux at the infant's skin, surface temperature of the incubator walls, and airflow velocity inside the chamber Table 6.2.

**Table 6.2:** Summary of test parameters

| Hood design | Inlet temperature (K) | Infant surface temp | Outlet & external wall temp | Turbulence model | Iterations | Diagnostics computed |
|---|---|---|---|---|---|---|
| Rectangular | 310 | Constant ~37 °C | Room temperature | k–ω SST (production limiter) | 1000 | Temperature contours; Convective heat-flux on skin; External-wall temperature; Pathlines & velocity vectors; Average velocity |
| Semi-circular | | | | | | |
| Trapezoidal | | | | | | |
| Rectangular | 315 | | | | | |
| Semicircular | | | | | | |
| Trapezoidal | | | | | | |

### 6.3.1 Thermal Distribution at 310K

Figure 6.9 shows how hood shape affects airflow and temperature. The rectangular hood causes uneven heating, the semicircular hood gives the most even temperature, and the trapezoidal hood creates unbalanced airflow inside the incubator.

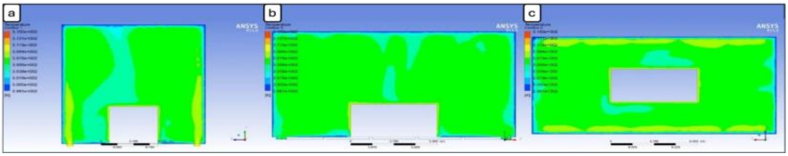

(a)

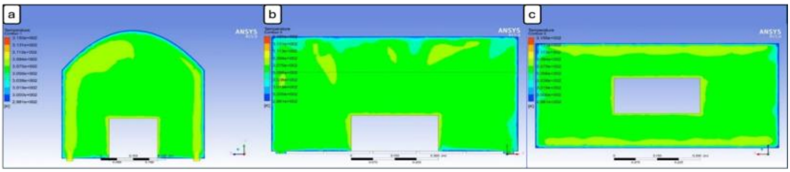

(b)

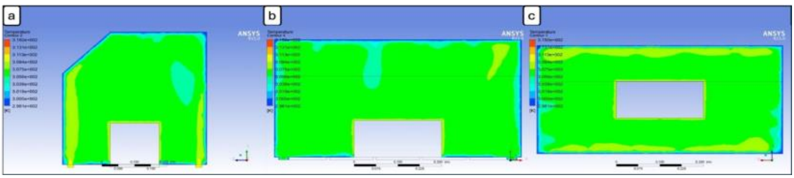

(c)

**Figure 6.9:** (a) Temperature distribution for rectangular hood at 310 K within an infant incubator; (b) Temperature distribution for semicircular hood at 310 K within an infant incubator; (c)

Temperature distribution for semicircular hood at 310 K within an infant incubator along (a) X-axis, (b) Z-axis, and (c) Y-axis.

At an inlet temperature of 310 K, the rectangular design demonstrated moderate uniformity in skin surface temperature. The airflow circulated primarily along the chamber walls, creating localized regions of higher velocity around the infant's head and feet. Temperature contours indicated uneven heating, with warmer zones concentrated near the inlet region, as shown. The semicircular configuration provided improved thermal uniformity compared with the rectangular design. The rounded geometry promoted smoother circulation patterns and minimized stagnation zones. Heat flux on the infant's surface was more evenly distributed, reducing hot and cold spots. The trapezoidal design produced intermediate results. Although airflow was directed more centrally than in the rectangular hood, the geometry generated asymmetrical flow paths that led to uneven heat transfer on the infant's torso. Velocity plots showed increased turbulence near the outlet, reducing thermal stability.

### 6.3.2 Thermal Distribution at 315K

Figure 6.10 shows the temperature behavior for different hood shapes. The rectangular hood increases temperature differences across the chamber, the semicircular hood maintains steady and even heat transfer, and the trapezoidal hood shows some improvement but still has minor airflow instability. The trapezoidal design showed some improvement at 315 K compared with 310 K, but uneven circulation persisted. Higher velocity jets near the outlet created localized areas of increased convective heat loss.

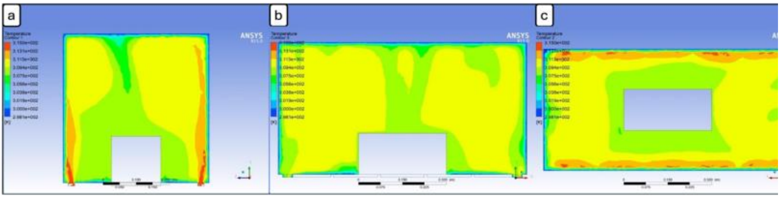

(a)

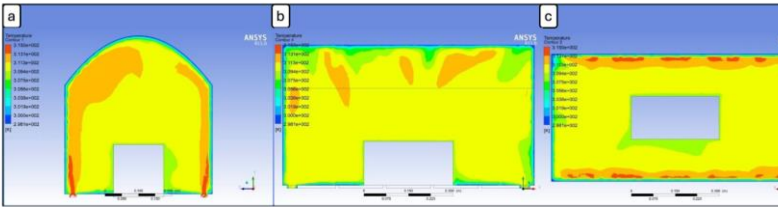

(b)

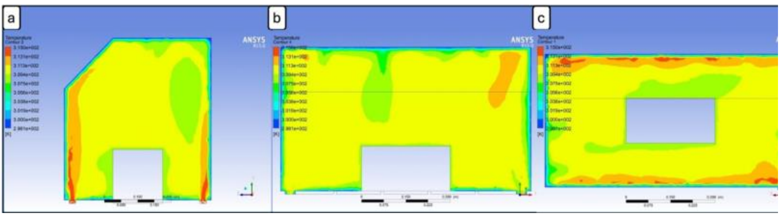

(c)

**Figure 6.10:** (a) Temperature distribution for rectangular hood at 315 K within an infant incubator; (b) Temperature distribution for rectangular hood at 315 K within an infant incubator; (c) Temperature distribution for trapezoidal hood at 315 K within an infant incubator along (a) X-axis, (b) Z-axis, and (c) Y-axis

### 6.3.3 Velocity Field Analysis

To quantify airflow distribution, the average air velocities were compared across designs. Results indicate that the semicircular hood maintained the most consistent velocity profile, with fewer fluctuations along the chamber length. In contrast, the rectangular and trapezoidal hoods exhibited greater velocity variations, contributing to uneven temperature fields Figure 6.11. Measured averages: a) Rectangular 0.364 $m \cdot s^{-1}$, b) Semicircular 0.309 $m \cdot s^{-1}$, c) Trapezoidal 0.358 $m \cdot s^{-1}$.

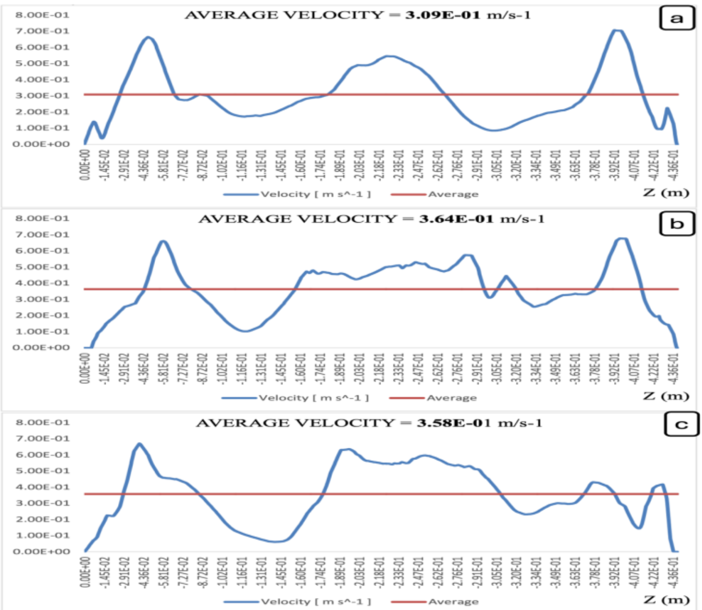


**Figure 6.11** Average velocity comparison for three hood designs

### 6.3.4 Comparative Discussion of Hood Designs

Across all geometries, the supply jet established a primary recirculation above the infant with smaller eddies near corners and around the head and shoulders—features that shape local convective losses. Recent CFD/manikin work indicates that enclosure-scale patterns are governed more by geometry and air-temperature set-point than by modest changes in inlet momentum; hotter supply air can reduce net convective loss but will intensify local gradients if jets impinge on exposed regions [16]. In our simulations, the semicircular hood's smooth curvature damped corner eddies and stabilized the velocity field, consistent with this evidence. Because thermoneutrality depends on both the air field and the mean radiant temperature, operative temperature (air + radiation) is the relevant control variable; designs that flatten wall/junction hot cold spots therefore improve skin-temperature uniformity. The semicircular hood produced the most even temperature field at both set-points, aligning with recent experimental and modeling findings [17]. Raising the inlet temperature increased overall heating in all designs but magnified non-uniformities in the rectangular and trapezoidal hoods, again matching reports that hotter supply deepens gradients when geometry steers flow toward the infant whereas the semicircular hood remained comparatively stable [18].

Operational features matter as well: transport-incubator studies show that opening access ports depresses internal temperature, while covers preserve central temperature but can create vertical stratification (warmer upper/posterior, cooler lower/anterior), underscoring a design–control trade-off that favors pairing port covers with guided return paths or diffusers [20]. From these insights, three practical guidelines follow: (i) adopt smooth internal curvature to suppress corner vortices and drafts; (ii) avoid direct jet impingement on the face/torso through inlet–outlet placement and diffusion; and (iii) prioritize radiant-field uniformity over high forced convection. Modern thermoelectric actuation and model-based control complement these geometric choices by tightening temperature regulation and lowering acoustic/vibration loads [21]. Consistent with the above, our comparative results across two set-points (310 K, 315 K) showed the semicircular hood delivering the most uniform skin-temperature field and the most stable internal velocity profile, the rectangular hood exhibiting inlet-side warming with corner-driven recirculation, and the trapezoidal hood yielding intermediate but asymmetric flow. Quantitatively, average internal velocities were ~0.309 $m \cdot s^{-1}$ (semicircular), 0.364 $m \cdot s^{-1}$ (rectangular), and 0.358 $m \cdot s^{-1}$ (trapezoidal), reinforcing that rounded internal geometry and non-impinging jet paths are first-order drivers of thermal uniformity in closed incubators.

## 6.4 CONCLUSION AND RECOMMENDATIONS

This work demonstrates that incubator thermal performance is governed by the coupled organization of airflow and radiation within the hooded enclosure. A controlled CAD-CFD workflow (SolidWorks geometry; ANSYS Fluent, SST k–ω with production limiter) was used to compare rectangular, semicircular, and trapezoidal hoods under clinically relevant set-points (air inlet 310 K and 315 K), with outlet and external walls at room temperature and steady solutions advanced to 1000 iterations. The comparative simulations show that interior curvature is a first-order design variable: the semicircular hood consistently suppressed corner recirculation and stabilized the internal velocity field, producing more even infant-surface temperature distributions at both set-points, whereas the rectangular hood exhibited inlet-side warming with stronger corner-driven eddies and the trapezoidal hood showed intermediate, asymmetric flow.

Quantitatively, the average internal velocities were ~0.309 $m \cdot s^{-1}$, 0.364 $m \cdot s^{-1}$, and 0.358 $m \cdot s^{-1}$ across the three designs (semicircular, rectangular, trapezoidal, respectively), supporting selection of the semicircular profile as the most efficient configuration for uniform heat transfer. These findings align with the thesis synthesis that outer-surface design directly steers internal airflow and heat loss, and they motivate practical recommendations on rounded hood geometry, non-impinging supply/return paths, and access-port management to reduce temperature non-uniformity and draft risk. While the present analysis focuses on dry convective/radiative conditions under steady operation, the methodology can be extended in future work to include evaporative fluxes, transient port openings, and alternative actuation (e.g., thermoelectric modules) within the same validated modelling framework. Such extensions are expected to reduce chamber energy demand and device mass further while improving tracking stability-directions already outlined for subsequent design iterations.

## 6.5 ACKNOWLEDGEMENT

The authors thank to the Universiti Teknologi Malaysia (UTM) for practical support.

# BIBLIOGRAPHY

[1] D. K. Baghel, S. L. Sinha, and S. K. Dewangan, “SST k–ω based air-flow and heat-transfer assessment in an infant incubator,” J. Comput. Appl. Res. Mech. Eng., vol. 12, no. 2, pp. 161–175, 2023.

[2] H. E. Belsinger Jr., U.S. Patent 6,428,465, 2002.

[3] Y. A. Çengel, Heat Transfer: A Practical Approach, McGraw-Hill, 1998.

[4] S. Delanaud, F. C. Yassin, E. Durand, P. Tourneux, and J. P. Libert, “Can mathematical models of body heat exchanges accurately predict thermal stress in premature neonates?,” Appl. Sci., vol. 9, no. 8, Art. no. 1541, 2019.

[5] Fluent Inc., FLUENT Product Documentation, 2000. [Online]. Available: https://www.fluent.com/documentation

[6] A. Fraguela, F. D. Matlalcuatzi, and Á. M. Ramos, “Mathematical modelling of thermoregulation processes for premature infants in closed convectively heated incubators,” Comput. Biol. Med., vol. 57, pp. 159–172, 2015.

[7] T. Fukuyama and T. Arimitsu, “Use of access port covers in transport incubators to improve thermoregulation during neonatal transport,” Sci. Rep., vol. 13, Art. no. 3132, 2023.

[8] S. Y. Gibbon, U.S. Patent 2,648,327, 1953.

[9] M. K. Ginalski, A. J. Nowak, and L. C. Wróbel, “A combined study of heat and mass transfer in an infant incubator with an overhead screen,” Med. Eng. Phys., vol. 29, no. 5, pp. 531–541, 2007.

[10] A. C. Guyton, Textbook of Medical Physiology, W. B. Saunders, 1986.

[11] A. Hannouch, C. Habchi, T. Lemenand, and K. Khoury, "Numerical evaluation of the convective and radiative heat-transfer coefficients for preterm neonate body segments inside an incubator," Build. Environ., vol. 185, Art. no. 107085, 2020.

[12] A. Hannouch, C. Habchi, N. Metni, and T. Lemenand, "Thermal analysis of a 3D-printed thermal manikin inside an infant incubator," Int. J. Therm. Sci., vol. 183, Art. no. 107826, 2023.

[13] E. N. Hey and L. E. Mount, "Heat losses from babies in incubators," Arch. Dis. Child., vol. 42, pp. 75–80, 1967.

[14] Y. H. Kim, C. H. Kwon, and S. C. Yoo, "Experimental and numerical studies on convective heat transfer in a neonatal incubator," Med. Biol. Eng. Comput., vol. 40, no. 1, pp. 114–121, 2002.

[15] H. Kobayashi, G. Tanaka, and T. Arimitsu, "Advanced thermoregulation by access port covers in neonatal transport incubators: Computational fluid dynamics analysis," J. Perinatol., 2025.

[16] A. J. Lyon and C. Oxley, "HeatBalance, a computer program to determine optimum incubator air temperature and humidity: A comparison against nurse settings for infants less than 29 weeks gestation," Early Hum. Dev., vol. 62, no. 1, pp. 33–41, 2001.

[17] A. Lyon and P. Puschner, Thermo Monitoring, Dragwerk AG, 1998.

[18] S. Murakami, S. Kato, and J. Zeng, "Combined simulation of airflow, radiation and moisture transport for heat release from a human body," Build. Environ., vol. 35, no. 6, pp. 489–500, 2000.

[19] C. B. Pereira et al., “Thermoregulation in premature infants: A mathematical model,” J. Therm. Biol., 2016.

[20] J. M. Rennie and N. R. C. Roberton, A Manual of Neonatal Intensive Care, Arnold Hodder, 2002.

[21] A. Rincón Casado, M. Larrodé-Díaz, F. Fernández Zacarías, and R. Hernández Molina, “Experimental and computational model for a neonatal incubator with thermoelectric conditioning system,” Energies, vol. 14, no. 17, Art. no. 5278, 2021.

[22] M. Rojczyk and I. Szczygieł, “Numerical and experimental analysis of infant radiant warmer,” in Proc. Conf., May 9–12, 2011.

[23] F. L. Strand, Physiology—A Regulatory System Approach, Collier Macmillan, 1980.

[24] H. K. Versteeg and W. Malalasekera, The Finite Volume Method: An Introduction to Computational Fluid Dynamics, 1995.

[25] J. Wasner, Heat Balance of Premature Infants, Dragwerk AG, 1994.

[26] World Health Organization, “Thermal control of the newborn: A practical guide,” WHO Meeting Report, Geneva, Switzerland, Apr. 8–10, 1992.

[27] O. Yeler and M. F. Köseoğlu, “Performance prediction modeling of a premature baby incubator having modular thermoelectric heat pump system,” Appl. Therm. Eng., vol. 182, Art. no. 116036, 2021